Bi©hemistry

pubs.acs.org/biochemistry Article

B-box1 Domain of MID1 Interacts with the Ube2D1 E2 Enzyme Differently Than RING E3 Ligases

Anupreet Kaur, Erin M. Gladu, Katharine M. Wright, Jessica A. Webb, and Michael A. Massiah*



Cite This: Biochemistry 2023, 62, 1012-1025



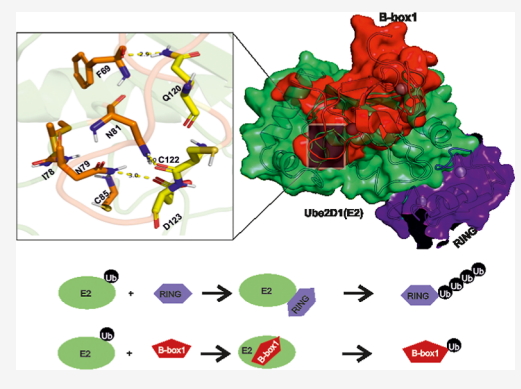
ACCESS

III Metrics & More

Article Recommendations

s Supporting Information

ABSTRACT: The MID1 TRIM protein is important for ventral midline development in vertebrates, and mutations of its B-box1 domain result in several birth defects. The B-box1 domain of the human MID1 protein binds two zinc atoms and adopt a similar ββα-RING structure. This domain is required for the efficient ubiquitination of protein phosphatase 2A, alpha4, and fused kinase. Considering the structural similarity, the MID1 B-box1 domain exhibits monoautoubiquitination activity, in contrast to poly-autoubiquitination observed for RING E3 ligases. To understand its mechanism of action, the interaction of the B-box1 domain with Ube2D1 (UbcH5a, E2), a preferred E2 ligase, is investigated. Using isothermal titration calorimetry, the MID1 RING and B-box1 domains were observed to have similar binding affinities with the Ube2D1 protein. However, NMR 15 N $^{-1}$ H Heteronuclear Single Quantum Coherence titration, 15 N relaxation data, and High Ambiguity Driven protein—protein



<u>DOCK</u>ing (HADDOCK) calculations show the B-box1 domain binding on a surface distinct from where RING domains bind. The novel binding interaction shows the B-box1 domain partially overlapping the noncovalent Ube2D1 and a ubiquitin binding site that is necessary for poly-autoubiquitination activity. The B-box1 domain also displaces the ubiquitin from the Ube2D1 protein. These studies reveal a novel binding interaction between the zinc-binding $\beta\beta\alpha$ -fold B-box1 domain and the Ube2D enzyme family and that this difference in binding, compared to RING E3 ligases, provides a rationale for its auto-monoubiquitination E3 ligase activity.

INTRODUCTION

X-linked Opitz G syndrome (XLOS) is an inherited disorder primarily associated with the mutation of MID1, and this is linked to ventral midline defects such as hypertelorism, cleft lip/palate, hyperspadias, and brain abnormalities. 1-3 MID1 (TRIM18) is a member of the <u>tri</u>partite <u>m</u>otif (TRIM) family of proteins characterized by their N-terminal tripartite RING-B-box-coiled coil domains. MID1 functions as an ubiquitin (Ub) E3 ligase catalyzing the poly-ubiquitination (polyUb) of protein phosphatase 2A (PP2A), alpha4, and the fused kinase. 3,5,6 PP2A functions as a molecular master switch, reversing the effects of phosphorylation initiated by kinases and thus regulates processes associated with metabolism, cell cycle progression, and apoptosis.⁷⁻¹¹ The protein alpha4 is an oncogenic protein and a regulatory subunit of PP2A within the target of rapamycin pathway that is important for regulating the cell cycle. 12-16 The fused Ser/Thr protein kinase plays a key role in the hedgehog signaling pathway and is involved in cell proliferation and patterning.

There are two types of B-box domains that are found mainly in TRIM proteins. The two types of B-box domains differ in length by 10–15 amino acids and do not share sequence homology with each other or with RING domains. Despite these differences, each domain coordinates two zinc ions and adopts a $\beta\beta\alpha$ -fold, similar to RING domains (Figure 1). In addition, the B-box1 domain is also found in the BBX family

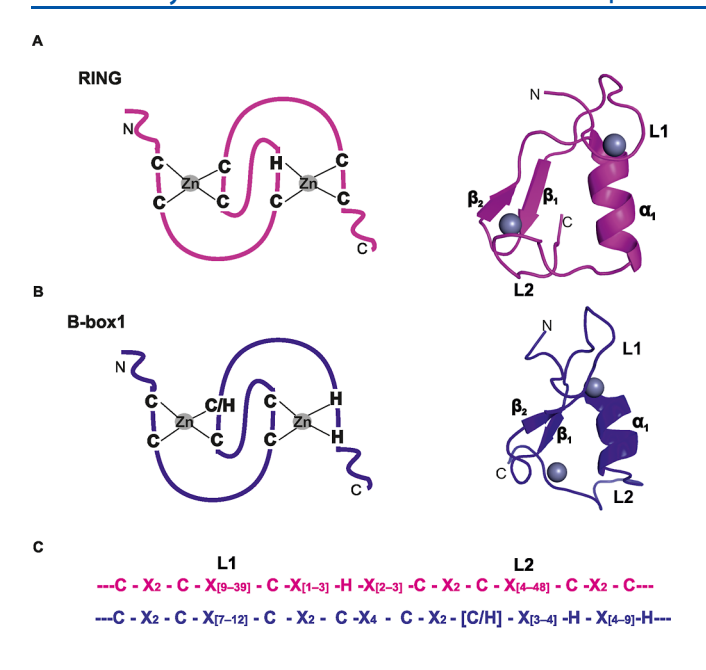
of plant transcription factors. 4,21,22 Very little is known about the mechanism of function of the B-box domains in the ubiquitination pathway.

Ubiquitin E3 ligase (E3) is one of three classes of enzymes involved in the RING-class-mediated protein ubiquitination cascades. Target proteins are covalently modified with a small highly stable protein called ubiquitin (Ub). Typically, the ubiquitinated protein is targeted to the proteasome for proteolysis. The first step in protein ubiquitination involves the E1 enzyme catalyzing the adenylation of the C-terminal glycine of Ub, followed by a nucleophilic attack by the sulfhydryl group of its active site cysteine in an ATP-dependent manner. The Ub is then transferred via a transthiolyation reaction to the active site cysteine residue of an E2 enzyme. Typically, E2 enzymes require the concerted action of an E3 ligase for substrate targeting and ubiquitination. RING E3 ligases represent the larger of two classes of E3 ligases, and they bind both the E2 and target proteins, acting as a scaffold

Received: December 9, 2022 Revised: January 30, 2023 Published: February 23, 2023







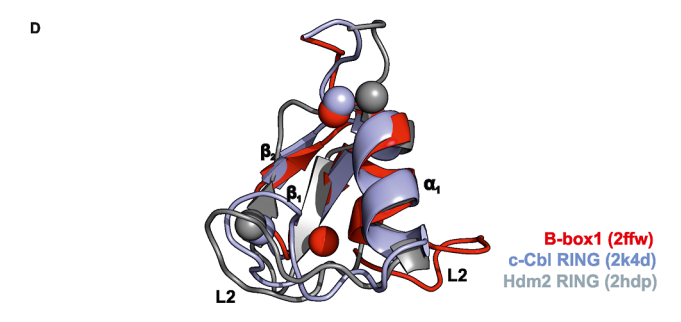


Figure 1. Zinc binding and structures of RING and B-box1 domains. Cross-brace zinc-binding mechanism by cysteine/histidine-rich sequences of (A) RING and (B) B-box1 domains. Ribbon representation of the Hdm2 RING domain (PDB: 2HDP) and the MID1 B-box1 domain (PDB: 2FFW). Both structures show the presence of two bound zinc ions (gray spheres) with a common $\beta\beta\alpha$ -RING fold. The α -helix of RING domains usually consists of two to three helical turns. (C) Sequence alignment of RING and B-box1 domains shows that the numbers of amino acids between zinc binding pairs are different. (D) Structural overlap of the MID1 B-box1 domain (PDB: 2FFW, red) with the E3 ubiquitin ligase c-Cbl RING domain (PDB: 2K4D, light blue, rmsd = 1.5 Å) and the Hdm2 RING domain (PDB: 2HDP, gray, rmsd = 2.3 Å). The position of the first zinc ion near the N-terminus of the helix is similar between the RING and Bbox1 domains, but the second zinc of the B-box1 domain is positioned at 3-4 Å.

to facilitate ubiquitin transfer. The side-chain e-amino group of a lysine of the target protein forms an isopeptide bond with the C-terminal carboxylate group of Ub.^{25,27} Subsequently, Ub can be added to other lysine residues on the target protein or onto the growing Ub chain.²⁵

It is generally accepted that the E2/E3 interaction is important for substrate ubiquitination. There are several structures of E2/RING E3 complexes, all showing a relatively conserved binding interaction. The structures reveal the RING domain is located approximately 15 Å away from the active site cysteine, suggesting that RING E3 ligases exert an allosteric effect toward the transfer of Ub. Supporting this hypothesis, mutational analyses of key residues at the E2/E3 interface and residues important for activation of the E2–Ub

thioester bond disrupts ubiquitin release from the E2 with the autoubiqutination (autoUb) assays.³⁷

Unlike the autoUb activities commonly observed for RING domains in the literature that shows a smearing pattern of high-molecular-weight polyubiquitinated products, the MID1 B-box1 domain exhibits auto-monoubiquitination (monoUb) activity. In this article, we present binding data that shows the MID1 B-box1 domain interacting with the Ube2D1 enzyme on a different surface compared with RING E3 ligase domains. The significance of this new binding interaction is unclear, but it provides an explanation for the auto-monoUb E3 ligase activity observed for the B-box1 domain.

MATERIALS AND METHODS

Cloning and Purification of B-box1 and Ube2D1. The B-box1 domain (residues 110–164) was previously cloned from the cDNA of the human MID1 gene by PCR into the pETite vector as C-terminal His₆-tagged proteins. The plasmid (pET30a) for the Ube2D1 (aka UbcH5a) protein was a gift from Dr. Ronald Hays of the University of Dundee (Scotland, UK). Page 10–16.

For ubiquitination reactions, the Ube2D1 (UbcHSa) and Bbox1 proteins were produced in *Escherichia coli* grown in LB medium and induced with 1 mM isopropyl β -D-1-thiogalactopyranoside for 3 h at 37 °C. Ube2D1 cells were harvested and resuspended in 50 mM Tris (pH 7.5), 1 mM EDTA, 1% Triton X-100, 5 mM DTT, and 2 mM PMSF and lysed by sonication. The Bbox1 cells were resuspended in 50 mM TRIS (pH 8.0), 200 mM NaCl, 20 mM β -mercaptoethanol (β -ME), and 1 mM ZnCl₂ and lysed by sonication. The lysates were centrifuged for 20 min at 20,000g, and the Ube2D1 and B-box1 proteins were purified by standard Ni²⁺-NTA affinity chromatography.

To obtain isotopically labeled Ube2D1 (E2) and Bbox1 proteins for NMR studies, the same protocol was followed as above except that cells were grown in M9 minimal medium supplemented with $^{15}\mathrm{NH_4Cl.}$

In Vitro Ubiquitination Assays. Lysine reactivity assays (thiolysis) were performed in a total volume of 100 μ L containing 0.6 μ M E1, 5 μ M E2 (Ube2D1), and 1 μ M HAtagged ubiquitin (HA-Ub) in 50 mM Tris-HCl (pH 7.5), 1 mM DTT, and 5 mM ATP-Mg²⁺. E2-Ub charging was performed for 30 min at 37 $^{\circ}$ C in the absence of the RING and B-box1 domain. ^{40,41} After charging, 50 mM of free lysine and 45 μ M of MID1 B-box1 were added. In a parallel control experiment, 45 µM of MID1 RING domain was added to a separate E2-Ub charged reaction. Samples were taken at specific time intervals and terminated with a nonreducing 2× sodium dodecyl sulfate-polyacrylamide gel electrophoresis (SDS-PAGE) sample loading buffer. The samples were analyzed by 15% SDS-PAGE and chemiluminescent Western blot using the antibody specific to HA-Ub. Experiments were performed in triplicates, and PVDF membranes were scanned with a G:BOX Chemi XX6 gel doc system (Syngene, Cambridge, UK). Scans were converted to gray scale, and the E2-Ub band was integrated as described.

Auto-ubiquitination assay reactions were performed in a total volume of 60 μ L at 37 °C. The reaction solution consisted of 0.7 mM DTT, 5 mM ATP-Mg²⁺, 0.2 μ M E1, 5 μ M E2 (Ube2D1), three different concentrations (i.e., 5, 25, and 50 μ M) of RING or B-box1 domains, and 5 μ M HA-tagged Ub in 50 mM Tris-HCl (pH 7.5). For time-course experiments, the reactions were stopped with 2× nonreducing

SDS-PAGE sample loading buffer and boiled at 90 °C for 5 min. Autoubiquitination E3 products were detected by analyzing the samples on a 15% SDS-PAGE gel followed by Western blot analyses.

Isothermal Titration Calorimetry of MID1 RING and Bbox1 Domain with Ube2D1. Isothermal titration calorimetry (ITC) studies were performed on a VP-ITC (MicroCal, Inc.,Northampton, U.S.A). All protein samples were dialyzed in 1× ITC buffer [20 mM sodium phosphate (pH 8.0) and 150 mM NaCl]. The B-box1 or RING domain concentration used in cells was 25 μ M, and 250 μ M Ube2D1 was titrated in a series of 25 μ L injections from the syringe with constant stirring at 310 rpm. Each injection was separated by 3 min intervals to equilibrate the system. As a control experiment, the $K_{\rm d}$ of Ub and Ube2D1 was measured by ITC to validate the MID1 RING and B-box1 binding constants. With ITC, 25 μ M Ub was titrated with 500 μ M Ube2D1, which were performed under similar conditions. Raw data were processed with the MicroCal Concat ITC software and then analyzed using Origin.

NMR Chemical Shift Perturbation Studies of Ube2D1 and the B-box1 Domain. NMR data were acquired at 15 °C using a Varian DD2 600 MHz spectrometer equipped with a 5 mm room temperature triple resonance probe with a z-axis gradient. All protein samples were prepared in 50 mM Tris (pH 7.5), 150 mM NaCl, 20 mM β -ME, and 0.1 mM ZnCl₂. Protein binding was monitored by chemical shift changes of signals from the $^{1}\text{H}-^{15}\text{N}$ heteronuclear single quantum coherence (HSQC) spectra of 500 μ M $^{15}\text{N}-\text{Ube2D1}$ acquired in the presence of 0.0, 1.0, and 2.0 equiv of unlabeled B-box1 domain. Similarly, HSQC binding titrations were performed with 0.0, 1.0, 2.0, and 3.0 equiv of unlabeled Ube2D1 added to 500 μ M $^{15}\text{N}-\text{B-box1}$ domain. The NMR data were processed and analyzed using NMRPipe⁴⁴ and CcpNmr (2.3.1)⁴⁵ and Sparky, respectively.

Measurement of Relaxation Experiments of Free and B-box1-Bound Ube2D1. 15 N T_1 , T_2 , and heteronuclear NOE (nuclear overhauser effect) data were acquired for 15 N Ube2D1 in the absence and presence of the B-box1 domain at 600 MHz with a Varian DD2 spectrometer. Relaxation delays of 100, 200, 300, 400, 500, 600, 700, 900, and 1100 ms and 10, 30, 50, 70, 90, 110, 130, and 150 ms were used for T_1 and T_2 measurements, respectively. The data was processed with NMRPipe⁴⁴ and analyzed using NMRFAM Sparky.

¹⁵N–¹H HSQC Titration of Ubiquitin and Ube2D1. NMR HSQC spectra were acquired using ¹⁵N Ube2D1 in Tris buffer containing Ub or the B-box1 domain at 0.5, 1.0, and 2.0 M equiv. For chemical shift and peak intensity analysis, the ¹H–¹⁵N HSQC spectra were recorded with 128 points in the indirect dimension. Each spectrum was processed using NMRPipe and analyzed with CCPNMR (2.3.1)⁴⁵ and Sparky.⁴⁶

Modeling of Ube2D1 and B-box1 Complex Using High Ambiguity Driven protein—protein DOCKing. Models of the Ube2D1/B-box1 protein complex were calculated using the software High Ambiguity Driven protein—protein DOCKing (HADDOCK 2.4). The protein—protein DOCKing (HADDOCK 2.4). Input structures for the docking were the solution structure of MID1 B-box1 (PDB: 2FFW¹⁹) and the X-ray crystallographic structure of Ube2D1 (PDB: 1W4U). HADDOCK structure prediction requires input for active and passive residues. The modeling was based on amino acids with significant signal broadening due to strong binding as well as extensive chemical

shift perturbations (CSPs), which are active residue restraints. These amino acids are E20, F31, W33, K63, V67, F69, I78, N79, N81, C85, L86, L104, K63, Y74, N77, E122, and I106 in Ube2D1 and C119, Q120, D129, T136, V139, T149, K153, and I162 in the Bbox-1 domain. Amino acids showing more than average CSPs were used as passive residue restraints, and they include N11, L13, R15, S22, L89, S105, D117, I123, and Y134 in Ube2D1 and C122, D123, Q127, T133, K146, and H150 in the B-box1 domain. Tests were also run in which HADDOCK was allowed to pick its own passive amino acids based on the active residues chosen. All runs gave similar results. HADDOCK outputs are in clusters, each consisting of groups of predicted structures that have similar backbone root mean square deviation (rmsd) values. The structures from the various clusters are very similar but have varying Z-scores based on slight differences in orientation of the protein complex and violations associated with noncovalent interactions and solvent accessibility. 47,48 Typically, structures with the lowest Z-score are predicted to be the best representation of a protein complex based on the NMR data. The HADDOCK-predicted structures were analyzed by PDBsum. Ramachandran dihedral angle analyses were performed to verify that the structures of the complex were not distorted by the docking procedure.

RESULTS

E3 Ligase Activities of the MID1 B-box1 and RING Domains. Despite not sharing sequence homology with RING domains, the MID1 B-box1 domain adopts a similar overall RING $\beta\beta\alpha$ -fold (Figure 1). ^{49,50} Although the structures are not identical, the variations at the primary and tertiary levels between the RING and B-box1 domains are similar to those observed among RING E3 ligase domains.⁵¹ Structural alignments using macpymol between the MID1 B-box1 domain (PDB: 2FFW) and two RING domains that form complexes with Ube2D1 reveal rmsd values of 1.5 and 2.3 Å with the c-Cbl RING domain (PDB: 2K4D) and Hdm2 RING domain (PDB: 2HDP), respectively. Structural comparisons with rmsd < 2.5-3.0 Å are considered reasonable alignments. To understand the B-box1 function and to gain insight into the mechanism by which the E2/E3 interaction might impact substrate ubiquitination, ^{29,35,52,53} the interaction of the MID1 B-box1 domain and the Ube2D1 E2 conjugating enzyme is investigated.

As is routinely done to demonstrate RING-type E3 ligase activity, 54,55 autoUb assays were performed with MID1 B-box1 and MID1 RING domains. As shown in Figure 2A, the automonoUb product was observed with the B-box1 domain. The intensity of the band corresponding to the monoUb (Bbox1–Ub) product (Figure 2A) increased substantially when the reaction time was increased from 90 to 180 min. Despite the increase in the Bbox1–Ub₁ band, the amount of polyUb B-box1 domain products was either very small and/or not detectable.

In contrast, the auto-ubiquitinated products for the MID1 RING domain were those of polyubiquitination (Figure 2A). The consistency of observing auto-polyUb products with the MID1 RING domain ^{56,57} and auto-monoUb products with the B-box1 domain led us to conclude that, under our in vitro conditions, the B-box1 domain only facilitates auto-monoUb, in contrast to RING E3 ligases. ⁵⁴

To gain insight into the mechanism of function of the B-box1 domain, lysine reactivity (thiolysis) assays were

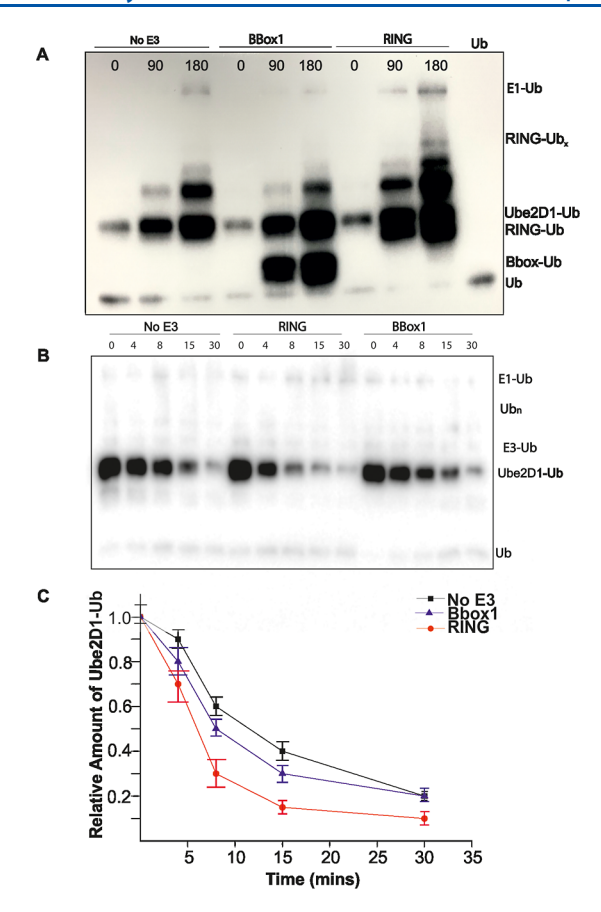


Figure 2. Ubiquitin E3 ligase activities of MID1 RING and B-box1 domains. (A) Western blot showing autoubiquitination assays of MID1 B-box1 and RING domains. (B) Western blot showing the lysine reactivity assay (thiolysis assay) of Ube2D1–Ub in the presence of B-box1 and RING domains. The E2–Ub band was subjected to nucleophilic attack by free lysine in the absence (control) and presence of each E3 ligase. The antibody was selective for HA–Ub in both blots. (C) Plots of the decrease in intensity of the E2–Ub bands over 30 min. Each point is based on the average values of three different trials.

performed. Given that RING domains bind distally from the E2–Ub thioester active site and exert allosteric effects on the transfer mechanism, we wanted to determine whether the monoUb activity was due to differences in allosteric effects. ^{41,52} As a control, breakage of the thioester Ube2D1–Ub bond is performed in the absence of RING or B-box1 domains.

Activation or allosteric exertion of the thioester linkages was confirmed using the lysine reactivity assays, for which the side-chain amino group of lysine serves as a good substitute for protein substrate. For these assays, the Ube2D1 enzyme was first charged with ubiquitin in the absence of an E3 ligase. After 30 min, the E3 ligase was added along with 100× molar excess of free lysine. The reactions were quenched at specific time points, and the disappearance of the E2–Ub band was tracked by chemiluminescent western blot (Figure 2B).

The assays revealed that in the absence of an E3 ligase, cleavage of the Ube2D1–Ub thioester linkage was relatively slow, as indicated by the gradual decrease in the band intensities (Figure 2C). In the presence of the B-box1 domain, thiolysis was faster, with an estimated 25% decrease in the E2–Ub band intensity at the 8 min time point compared with the control reaction, which showed only a 10% decrease (Figure 2C). In contrast, the MID1 RING domain yielded a greater

amount of Ube2D1—Ub cleavage, with most of the complex (>50%) gone at the 8 min mark (Figure 2C). These observations indicate that the interactions of the MID1 RING and B-box1 domains with Ube2D1 result in a different level or type of allosteric effect. We postulate that these two domains interact differently with the Ube2D1 enzyme.

Binding Affinity of Ube2D1 with the B-box1 and RING Domains. It is possible that the MID1 RING and Bbox1 domains bind with different affinities, and this may contribute to the differences in allosteric effects. To understand how the B-box1 domain might interact with Ube2D1, we measured the binding affinity. ITC experiments were performed, and the dissociation constants (K_d) between Ube2D1 and the RING and B-box1 domains were estimated to be 43 ± 9.4 and $34 \pm 10.2 \,\mu\text{M}$, respectively (Figure 3). The large error values for the K_d values may be due to the low solubility of the complex, which most likely prevents complex formation for a percentage of the E3 and B-box1 domains. 59-63 These K_d values indicate that the MID1 RING and B-box1 domains bind the Ube2D1 enzyme with similar affinities. Interestingly, the K_d values were also lower than those observed for other Ube2D-RING complexes, which are in the (100-250 μ M range). Our lower estimates of K_d values can be attributed to measuring technique but most likely due to differences in the E3 proteins. The $K_{\rm d}$ values for Ube2g2/RING⁶⁵ and Ube2D2/c-Cb1⁶⁴ complexes were measured using NMR spectroscopy and found to be 144.0 \pm 10 and 170.0 \pm 96 μ M, respectively. The K_d value of Ube2D2/ RNF38⁶⁶ complex was measured by SPR to be 89.0 \pm 1 μ M, while ITC was used to measure the Ube2D2/RNF13 and Ube2D2/RNF4 complexes to be 11.0 nM and 179.0 μ M, respectively.⁶⁷ The $\hat{K}_{\rm d}$ values of other pairs of the non-Ube2D¹⁻³ family of E2s with RING domains are shown to be in the sub-uM range. 43,64 To confirm that our values are not technique- and condition-specific, we measured the K_d value (Figure 3C) of Ube2D1 and Ub to be 190 \pm 57 μ M, and this value is similar to published data of 215 \pm 80 μ M. ^{68,69}

MID1 B-box1 Domain Interacts Closely with the C85 Active Site of Ube2D1. Given that MID1 RING and B-box1 domains interact with Ube2D1 with similar affinities but that thiolysis data suggest they exert different allosteric effects, we next used two-dimensional NMR spectroscopy to gain residuelevel insights into the binding interface. The 15N-1H HSQC spectra of the Ube2D1 enzyme and the Bbox1 domain were dispersed, and the ¹⁵N-¹H peak positions were consistent with what had previously been reported for these proteins (BMRB entries 6277 and 6920). 70,71 The noncovalent interaction was monitored by following the relative peak intensity and/or chemical shift changes of the ¹⁵N-labeled protein when titrated with unlabeled protein. To identify amino acids of Ube2D1 that are involved in binding, 15N-1H HSQC spectra of Ube2D1 were recorded in the absence of the B-box1 domain and with 1.0 and 2.0 M equiv. Titrations with more protein equivalences were prevented by protein precipitation. It is possible that the concentration of proteins used for NMR spectroscopy may have contributed to the formation of aggregates. Systematic changes were observed for several amino acids in the presence of the B-box1 domain. Figure 4A shows the overlay of the ¹⁵N-¹H HSQC spectra of free and Ube2D1 in the presence of 2.0 M equiv of the B-box1 domain. The signals for residues E20, F31, W33, K63, V67, F69, I78, N79, N81, C85, L86, and L104 of Ube2D1 were broadened by more than 80% of their original intensity. The broadening is

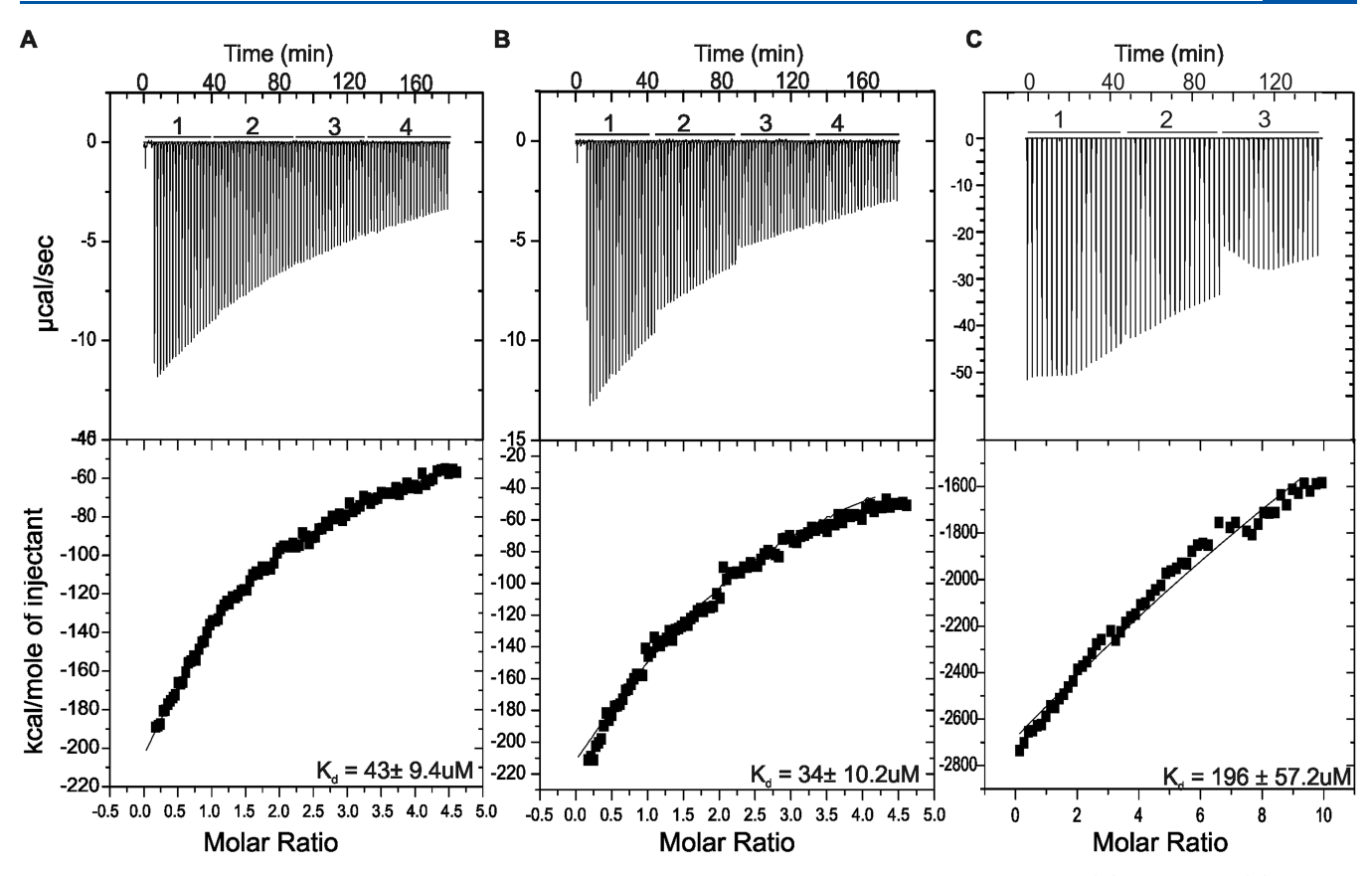


Figure 3. Isothermal calorimetry binding studies of E2 and cohort proteins. Binding ITC isotherms of MID1 RING (A) and B-box1 (B) domains and of ubiquitin (C) binding with Ube2D1 at 8 °C. Titrations were carried out in a Micro-ITC calorimeter in 20 mM sodium phosphate buffer (pH 8.0) containing 150 mM NaCl. Data were analyzed using the Origin software.

most likely due to the intermediate binding strength of the complex, which is consistent with the low μM binding affinity estimated by ITC. The broadening indicates two populations of Ube2D1, one in the unbound state and the other in the Bbox1-bound state, where the exchange rate between these two states is slow enough that each can be detected by NMR spectroscopy. Thus, at a 1:2 Ube2D1/B-box1 molar ratio, approximately 80% of the Ube2D1 was in a complex with the B-box1, and this complex is less mobile (hence broader peaks) than the unbound proteins (Figure 4A(i-v)). The residues affected most significantly are located near strand β 1, between β 3 and helix α 2, and the loop adjacent to the active site C85 cysteine residue (Figure 4B). In addition to signal broadening, the NH signals of several amino acids changed chemical shift (Figures 4A and 7A). In contrast of the magnitude of chemical shift changes reported for several RING domains with Ube2D1, 30,53,72,73 chemical shift changes (CSP) were relatively larger for the Ube2D1/B-box1 complex. It is possible that performing the NMR titration studies at 15 °C, as compared with 25 °C, slowed the fast exchange rate sufficiently to show the greater shifts and the broadening. Interestingly, the shift remained when the NMR sample was heated to 25 °C, suggesting the complex is stable. There are 17 peaks that shifted ($\overline{\text{CSP}} + \sigma$) and they include N11, L13, R15, S22, K63, A68, Y74, N77, N81, L89, L104, S105, I106, D117, E122, I123, and Y134. Of these, signals for residues K63, N81, L86, and L104, which are located near helix α 2, are also significantly broadened.⁷⁴ The amino acids that exhibit peak or signal broadening are localized on a specific surface of the Ube2D1 enzyme (Figure 4B),

To identify the amino acids of the B-box1 domain that are involved in binding, ¹⁵N-¹H HSQC spectra of the ¹⁵N-labeled B-box1 domain were acquired with 1 and 2 M equiv of the Ube2D1 enzyme (Figure 5A). Changes in NH peak intensities of signals and chemical shift changes induced are plotted and shown in Figure 5B. Amino acids that showed significant signal broadening are C119, Q120, D129, T136, V 139, T149, K154, and I162. Residues C122, D123, Q127, T133, and H150 exhibit CSP. These residues are located near β_1 , β_2 , and α helix. Though not the same amino acids, the locations of these residues are similar to those reported for RING domains that form complexes with the Ube2D1-3 enzyme family (Figure 5C). 29,30,33 However, the NMR data show these residues to bind the Ube2D1 enzyme at a different site (Figure 6). Amino acids of the Ube2D1 that are involved in binding RING domains⁷⁴ are localized near the N-terminal helix and loops spatially near this region (Figure 6A). The Ube2D1 the amino acids contacting the B-box1 domain are localized near the loop connecting helix α_3 and strands β_1 and β_3 (Figure 6B). We are unable to map the interaction of the MID1 RING domain with Ube2D1 to make a more direct comparison because the MID1 RING domain forms large soluble aggregates that do not yield NMR signals, and its titrations with Ube2D1 at NMR concentrations result in precipitation.

The overall similarity in chemical shifts of the N-H signals (Figures 4 and 5A) of the Ube2D1 and Bbox1 proteins in isolation and in complex indicate that the binding did not induce large changes in the secondary and tertiary structures of either protein.

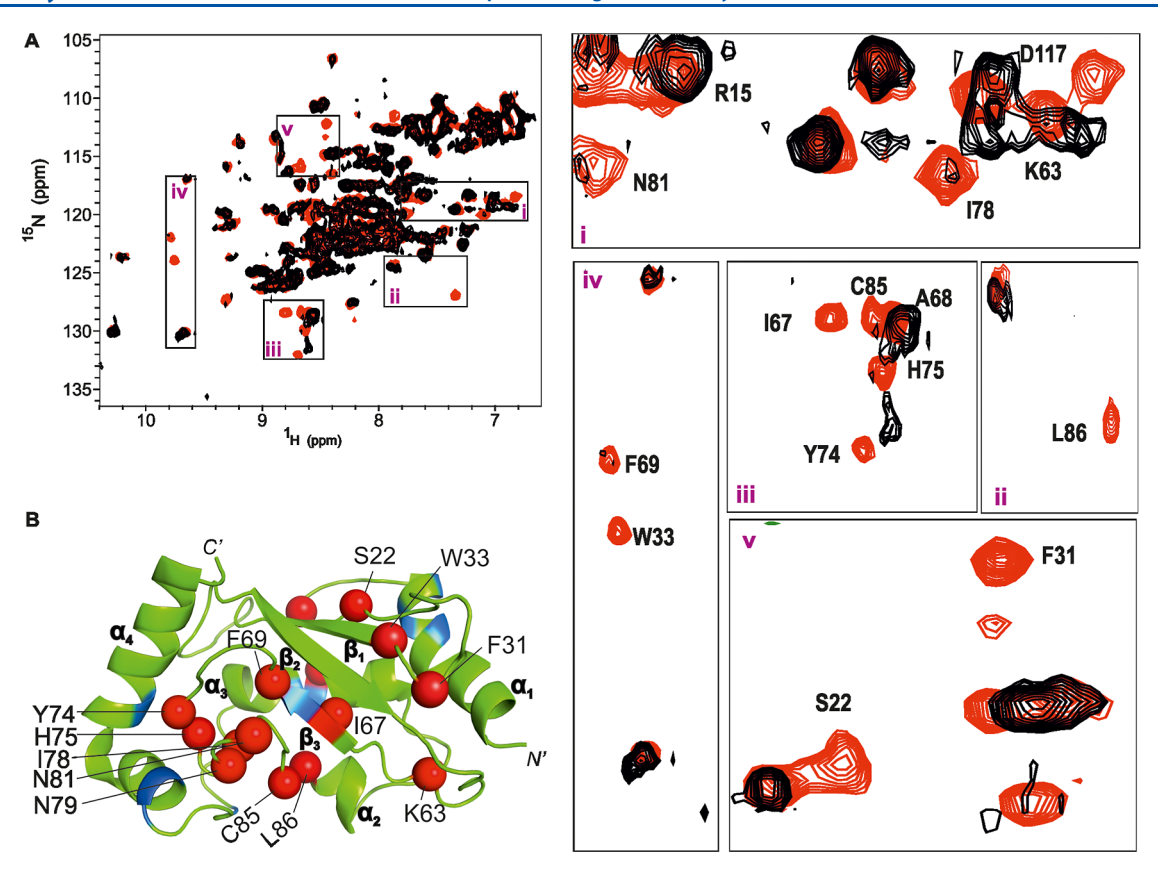


Figure 4. NMR binding studies of ¹⁵N-Ube2D1 and B-box1 domains. (A) ¹⁵N-¹H HSQC spectra of Ube2D1 recorded in Tris buffer in the absence of 0.0 M equiv (red) and in the presence of 2.0 M equiv (black) of the Bbox1 domain. (i-v) Zoomed-in regions of the ¹HSQC spectra show examples of peak broadening, as the predominated effect, and shifting. (B) Amino acids experiencing significant signal broadening and CSPs are highlighted as red and blue spheres, respectively.

NMR Backbone Relaxation Experiment Confirms Bbox1 Binding. ¹⁵N-relaxation data were used as an additional mechanism to confirm the interaction between the B-box1 and Ube2D1 proteins. T_1 , T_2 , and NOE properties of the NH bonds can provide insights in the dynamics properties (mobility) of residues in or near the binding interface (Figure 7 and S1). In general, lower T_1 and heteronuclear NOEs values and higher than average T2 values for amino acids indicate flexibility (Figure S1). Consistent with reported values, the Ube2D1 protein shows⁷⁵ more flexibility near strand β 1 and the loop connecting to $\alpha 2$ in the absence of the B-box1 domain. The relaxation data of Ube2g2 and Ubc13 also show dynamic properties near these regions, and it was concluded that ps-ns motions of these regions contribute to E2 catalytic activity. 70,75-77 The presence of the B-box1 domain resulted in increases and decreases in T_1 and T_2 values, respectively, for almost all Ube2D1 amino acids. An effective way to visualize changes in the backbone dynamics is to compare T_1 and T_2 values by using their reciprocal values, R_1 (1/ T_1) and R_2 (1/ T_2), respectively. If the R_2/R_1 values are the same for the free and B-box1-bound Ub2D1, it would indicate no effect on backbone dynamics and no binding. Several amino acids exhibit greater R_2/R_1 values, indicating that these residues have become more rigid. Residues that show the increased R_2/R_1 values are mapped to regions of the Ube2D1 secondary and tertiary structures that contact the B-box1 domain. These regions of Ub2D1 also consist of the amino acids that show CSP and signal broadening (Figure 7A). Similarly, the heteronuclear ¹⁵N-NOE values for most of the backbone

atoms of Ube2D1 show marked increases in values, confirming the binding interface and the overall increase in rigidity in the Ube2D1 protein when bound to the B-box1 domain (Figure 7C). We anticipate that qualitatively the pattern and magnitude of changes in R_1 , R_2 , and NOEs values may be different with RING domains, ⁷⁵ but we are unable to make such a comparison because of a lack of published data.

Structural Models of the B-box1 Domain–Ube2D1 Complex. With the identification of the interfacing residues, we modeled the complex using HADDOCK [31, 32, 48]. Amino acids showing significant broadening and extensive perturbation were used as restraints for the interface of the Ube2D1 and B-box1 protein complexes. Results of docking calculations are shown in Figure 8. The various models reveal a binding interaction that agrees with the NMR data. The top three HADDOCK structures (Figure 8A) have an average rmsd of 7.0 ± 0.4 , 6.4 ± 0.2 , and 4.8 ± 0.5 Å, respectively. These results suggest that the binding surface on Ube2D1 is effectively the same for all complexes. In all the models, the B-box1 domain is positioned over $\beta1$ and $\beta3$ strands of Ube2D1, but the orientation of the B-box1 domain differs between models, resulting in different Z-Scores and rmsd values.

According to HADDOCK, the best structure has the most negative Z-score and is listed as cluster 1, model 1. The model shows the B-box1 domain positioned near the active site C85 residue (Figures 6C and 8). The interfacing residues in model 1 were confirmed by analysis using the program PDBsum⁷⁸ and shown to consist of both hydrophobic and polar residues (Figure S2A). Residues F31, A68, F69, N79, and N81 of

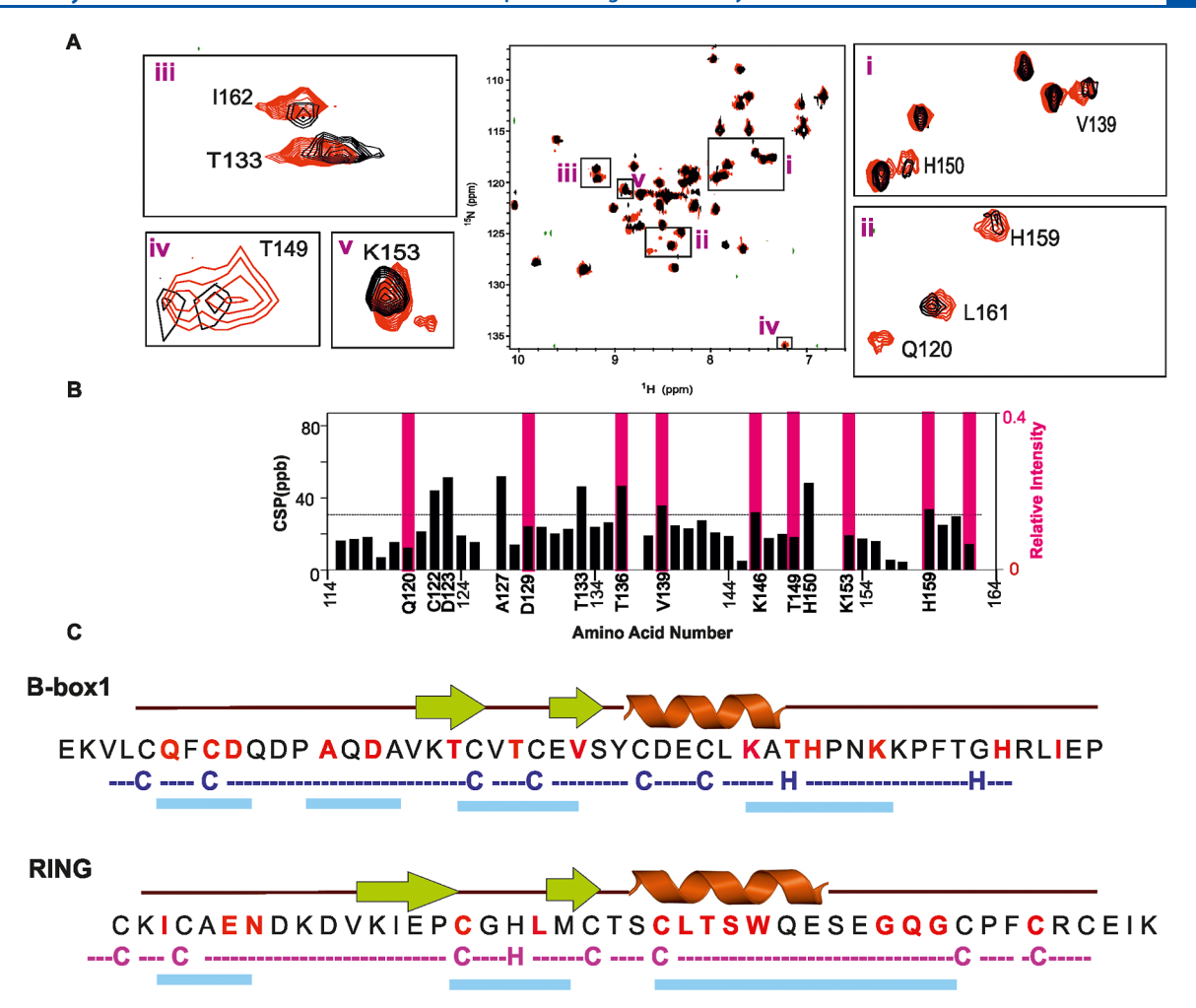


Figure 5. NMR binding studies of ¹⁵N-B-box1 and Ube2D1 domains. (A) ¹⁵N-¹H HSQC spectra of the ¹⁵N-labeled B-box1 domain in the absence of 0.0 M equiv (red) and in the presence of 2.0 M equiv (black) of unlabeled Ube2D1. Zoomed-in regions of the spectra show peaks of some backbone amides of Bbox1 affected by the binding of Ube2D1. (B) Relative peak intensity and CSP plots corresponding to amino acids of the ¹⁵N Bbox1 domain measured by comparing the spectra in the absence and in the presence of 2 M equiv of Ube2D1. (C) Structure and sequence alignment of RING and B-box1 domains representing similar regions of RING and B-box1 involved in interaction with Ube2D1 (regions are shown in cyan color).

Ube2D1 are near residues E120, D123, C122, and H159 of the B-box1 domain, which is consistent with the NMR data. The sidechain amide groups of asparagine N79 and N81 of Ube2D1 are near D123 (~2.70 and 3 Å, respectively) and C122 (3 Å) to form hydrogen bonds (Figure 8B(ii)). Hydrophobic stacking interaction is observed between F69, A68, and F31 of Ube2D1 and B-box1 Q120 and H159 amino acids (Figure 8B(i)). To validate the structures, a Ramachandran plot, calculated for model 1 using PROCHECK, shows 67, ~30, ~3, and ~0.5% residues in the most favored, additional allowed, generally allowed, and disallowed regions, respectively (Figure S2B). The observed g-factor of dihedral angles was ~0.38, indicating that docking did not distort the structure.

The B-Box1 Perturbs the Ube2D1–Ub Noncovalent Interaction. The HADDOCK model and NMR data reveal that the location of the B-box1 domain partially overlaps the surface where the noncovalent Ub has been shown to bind. The noncovalent Ub–Ube2D2 interaction is important to promote chain elongation and auto-polyUb products. In previous binding studies, residues D16, S22, Q34, F51, I78, L86, V102, and M147 of Ube2D1 are involved in binding with

the noncovalent Ub.⁶⁸ Hydrophobic residues L86, I78, and S22 are involved in interactions with both the B-box1 and Ub proteins (Figure 9). The modeling reveals that the B-box1 domain partially overlaps the noncovalent Ub binding site (Figure 9A).

To test whether the B-box1 domain would disrupt the interaction between Ube2D1 and Ub, the B-box1 domain was titrated into a 1:1 molar ¹⁵N-labeled Ube2D1 and Ub solution that was allowed to incubate to stabilize the complex. The HSQC spectrum of the Ube2D1-Ub complex is consistent with binding in a similar location, as reported.⁶⁸ Addition of the B-box1 domain induced CSP and broadening of Ube2D1 signals, which is consistent with free Ube2D1 (Figure 9B). These observations indicate that B-box1 domain, which binds stronger ($K_{\rm d~(Ube2D1-B-box1)} \sim 30~\mu{\rm M}$ and the $K_{\rm d~(Ube2D1-Ub)} \sim$ 200 uM),66 was able to displace the noncovalent Ub (Figure 9C). In contrast, when 1 M equiv of Ub was added to a 1:1 molar solution of Ube2D1 and the B-box1 domain, most of the Ube2D1 ¹⁵NH signals were unchanged (Figure S3). However, with 2 M equiv of Ub, almost all of the 15NH signals disappeared, consistent with Ube2D1 precipitation (Figure S3).

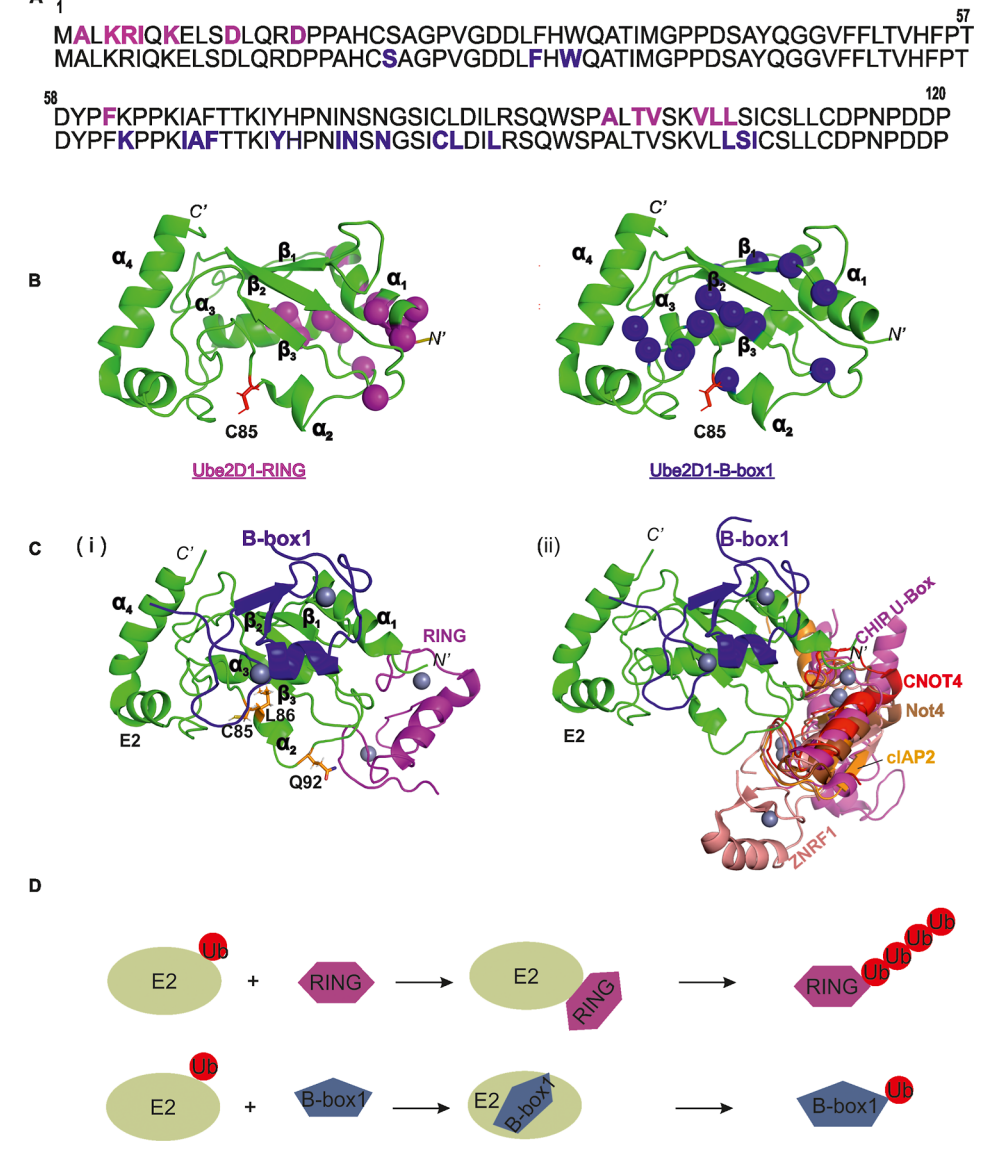


Figure 6. Structural comparison of RING and B-box1 binding sites on Ube2D1. A Sequence comparison of amino acids of Ube2D1 involved in binding with RING (pink, first row) and MID1 B-box1 (blue, second row) domains and these differences are highlighted with spheres in their respective colors in B. (B) Ribbon representation of Ube2D1 with the same orientation mapping the binding sites. (C) Structure representation showing the binding site of the MID1 B-box1 domain with Ube2D1. The site is different than the RING domain binding sites showing the (i) comparison with one RING domain and (ii) variations in the binding interaction. (D) Cartoon representation rationalizing how differences in binding RING domains and the MID1 B-box1 domain with the Ube2D1 enzyme may impact their level of autoubiquitination.

DISCUSSION

The B-box domains of TRIM proteins are shown to be essential for efficient ubiquitination of substrates.^{3,6} Their similar $\beta\beta\alpha$ -RING folds (Figures 1 and 2) and E3 ligase activity indicate that they may represent a new class of RING-type E3 ligases.^{5,19,20} Very little is known about how the B-box1 domain functions.

The NMR and modeling data reveal that the MID1 B-box1 domain binds the Ube2D1 enzyme at a distinct site from the prototypical E2/RING interface (Figure 6). Structures of RING bound to Ube2D1-3 show the RING domains positioned ~15 Å from catalytic C85 residue that forms the thioester bond with the C-terminal glycine of Ub (Figure 6C). In contrast, the B-box1 domain is positioned near strands β 1, β 3, and α -helix and ~5 Å from C85. Its presence induces rigidification of backbone motions for most Ube2D1 residues

(Figure S1). The total surface area of interaction is calculated to be \sim 615 Å², similar to the values of RING/E2 interfaces (\sim 563 \pm 27 Å). This difference in binding may provide a rationale for the differences in allosteric effects and the auto-Ub activities between the MID1 RING and B-Box1 domains (Figure 2A). The activation of the thioester linkage for nucleophilic attack, compared with the absence of any E3 ligase, supports the B-box1 domain as a RING-type E3 ligase.

It is unclear why the B-box1 domain binds on a different surface, given that its interfacing residues are on a similar surface as RING domains. It is possible that these residues of the B-box1 domain complement residues on this beta-sheet surface of the Ube2D1. However, we postulate that the location of loop2, which is different between RING domains and the B-box1 domain, influences the binding mechanism. MID1 B-box1 domain has a highly conserved proline residue

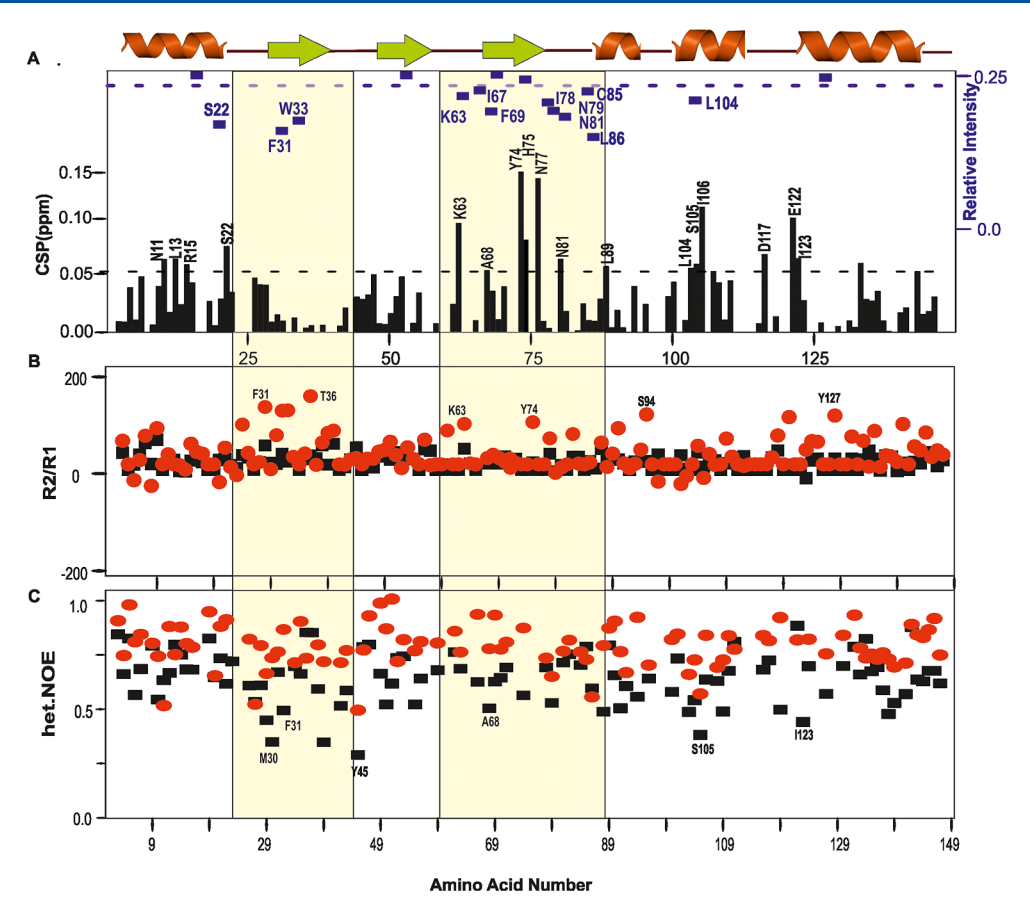


Figure 7. Relaxation and conformational data confirming B-box1 and E2 binding. (A) Relative peak intensity plot and CSP corresponding to all amino acids of Ube2D1 measured by comparing the peak intensity and position with the $^{1}H^{-15}N$ HSQC spectra in the absence and in the presence of 2.0 M equiv of the B-box1 domain. The ratio of ^{15}N R_2 (transverse relaxation rate) to ^{15}N R_1 (longitudinal relaxation rate), $^{1}H^{-15}N$ heteronuclear NOE for ^{15}N Ube2D1 in unbound (black) and bound to B-box1 (red) are shown. The data show the effect of B-box1 binding on the dynamic properties of residues in or near its binding site on Ube2D1. The putative regions of Ube2D1 involved in interaction with B-box1 based on $^{1}H^{-15}N$ HSQC titrations and relaxation experiments are highlighted with a yellow background. The secondary structural elements of Ube2D1 are labeled as α helix, β sheets, and coils, which are drawn on the top of the plots.

(P151) located at the end of the α -helix and beginning of loop 2 (see Figure 6A in ref 3 and Figure 5B³⁹). RING domains do not possess a proline residue at or near this junction. The rigid backbone structure of P151 positions loop 2 outward toward the outer surface of the α -helix (Figure 8B). In contrast, the amino acids of loop 2 of RING domains are positioned inward and contribute to intra- and intermolecular interactions. The inward positioning of loop2 with RING domains would sterically block the RING domain from interacting in a similar manner as the B-box1 domain.

In addition, the intermolecular interaction involving loop2 residues contributes to allosteric effects. For example, loop 2 usually consists of at least one lysine or arginine residue that is observed to form a hydrogen-bond interaction with residue Q92 on loop 7 of Ube2D1 and other similar E2s. Hatalian Mutations of Q92, structurally near C85, have been shown to disrupt the reactivity of the thioester linkage. The B-box1 domain contains two lysine residues on loop2, but the outward orientation places these residues far from Q92. Thus, the reduced allosteric effect could be explained by the lack of a hydrogen bond to Q92. Indeed, the HADDOCK structures of the Ube2D1/B-box1 complex show loop 2 positioned on the opposite side of Q92 on Ube2D1 (Figure 8B). Changing the orientation of loop 2 with the B-box1 domain could, in theory, promote interaction with Q92 and change the allosteric effect.

While not exactly clear, a XLOS-derived P151L mutant B-box1 domain exhibited significantly greater E3 ligase activity compared with the wildtype B-box1 domain.³⁹ Further structural and functional studies need to be performed to confirm this hypothesis.

It is conceivable that the binding mechanism and location of the two zinc ions in B-box1 and RING domains may contribute to E2 binding. Superposition of the MID1 B-box1 domain with RING domains show that the zin-ion near the Nterminus of the α -helix is positioned in close proximity, while the other, associated with loop 2 is separated by ~5 Å away from those of the RING domains (Figure 1D). This difference in the location of this second zinc ion is largely due to differences in the zinc coordination by the RING and B-box1 domains.⁸⁶ Supporting this argument, the locations of the two zinc atoms are more aligned and similar among the few B-box1 structures known. In all of the E2/RING complexes, the zinc ions play a purely structural role in stabilizing the structure and are not directly involved with the interaction of any amino acids of the E2 protein. Thus, other than the indirect structural role, the zinc ions do not influence E2/RING or E2/Bbox1 binding interactions. It should also be noted that by definition, zinc ions play a structural role in zinc-finger protein and removal of the zinc ions results in domain unfolding. Interestingly, the way the B-box1 domain binds to the Ube2D1

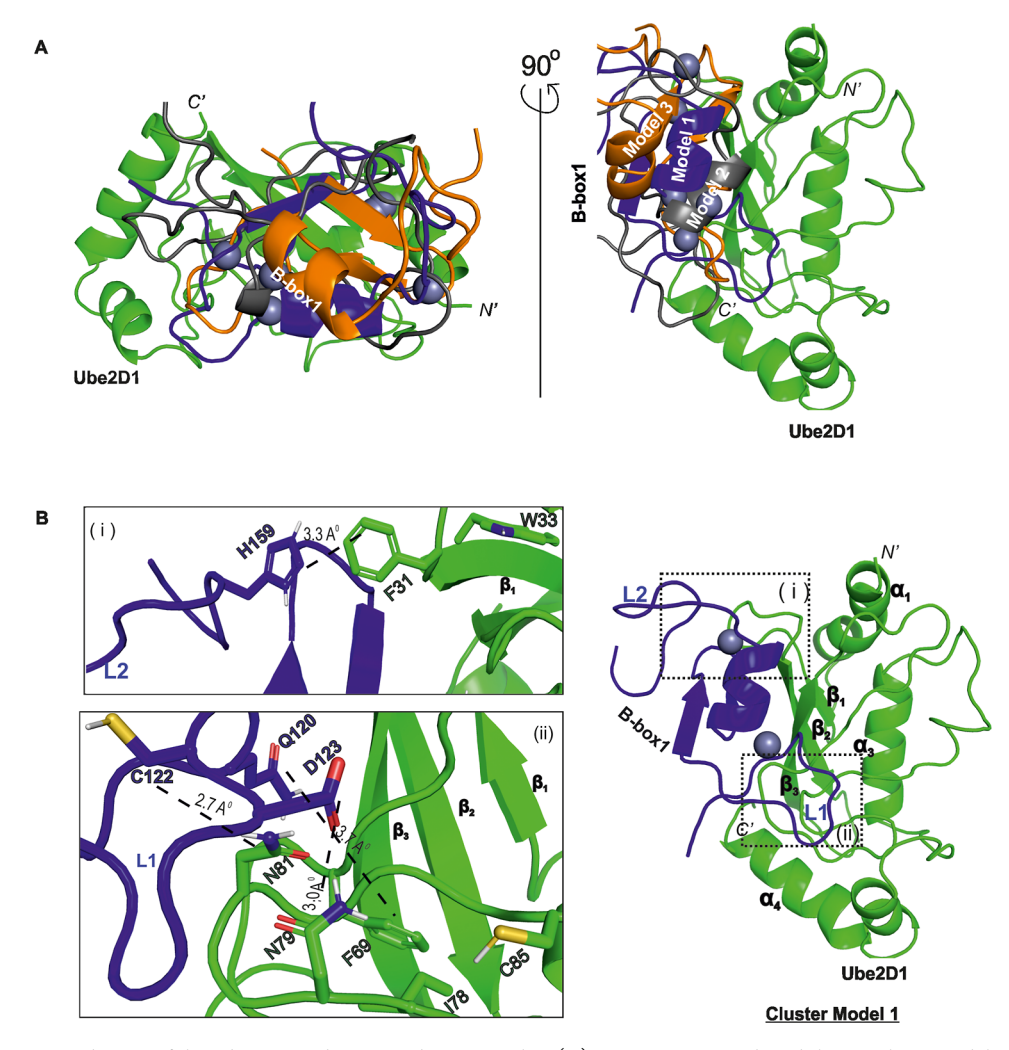


Figure 8. HADDOCK prediction of the Ube2D1 and MID1 B-box1 complex. (A) HADDOCK predicted the top three models (cluster model 1, Z-score = -1.9; cluster model 2, Z-score = -1.2; and cluster model 3, Z-score = -0.2) of Ube2D1 and the MID1 B-box1 domain. (B) Close-up view of a key region showing residues involved in noncovalent interactions with cluster model 1 and confirmed by PDBsum analysis.

enzyme could be rationalized to explain the auto-monoUb activity. As previously shown, noncovalent Ub binding to Ube2D2⁸² is essential for catalysis of poly-ubiquitinated products, or the high molecular weight bands depicted by the smearing pattern in western blot images (Figure 2). The Ub–Ube2D2 interaction involved key hydrophobic residues, particularly L86, I78, and S22 of the E2 enzyme. These residues are also involved in binding the B-box1 domain. ITC and NMR titrations show that the MID1 B-box1 domain binds Ube2D1 much tighter than Ub and displaces the bound Ub. This tighter binding and location would sterically block the Ub binding necessary to promote auto-monoubiquitination (Figures 2 and 9A).

Furthermore, the Ube2D1 and B-box1 binding mechanism may also affect how the covalently attached Ub interacts with Ube2D1, and this could affect the reactivity. Klevit et al. showed that the covalently attached Ub was highly mobile but appeared to sample two populations that are characterized as closed and open conformations. The closed conformation is important for access to the thioester linkage. Binding of the RING domain promotes the closed E2–Ub conformation, in which the Ub makes slightly greater contacts with residues near α -helix 2 of the E2 enzyme. In contrast, the tight binding of the B-box1 domain near the active site could

sterically hinder the closed conformation. This disruption might impact how quickly auto-monoUb products appear and possibly the chain elongation associated with polyUb (Figure 6D).

Finally, it is possible that the Ube2D1–B-box1 binding might reflect how E4 ligases interact with their cognate E2 enzymes. For example, BARD1 and MDMX are considered E4 ligases (E3-enhancing ligases) by forming heterodimers with BRCA1 and MDM2, 100 respectively, and enhancing the E3 ligase activity observed. Similarly, MID1 requires the tandem RING–B-box1 domains for optimal activity, such as autopolyubiquitination and the polyubiquitination of PP2A and alpha4. The B-box1 domain may play a similar role as BARD1 and MDMX within the BRCA1/BARD1 and MDM2/MDMX complexes. 100 representations of PP2A representations of PP2A representations of PP2A representations. 100 representations of PP2A repres

In summary, we used NMR and modeling to show that the MID1 B-box1 E3 ligase domain binds the Ube2D1 E2 enzyme differently than the prototypical RING E3 ligases. While the B-box1 domain does exhibit E3 ligase activity, this mechanism of binding may explain the auto-monoUb activity observed. It is unclear whether other B-box1 domains would interact with their cognate Ube2D1-3 enzymes in a similar manner, but we speculate that the conserved proline just preceding loop2 in B-

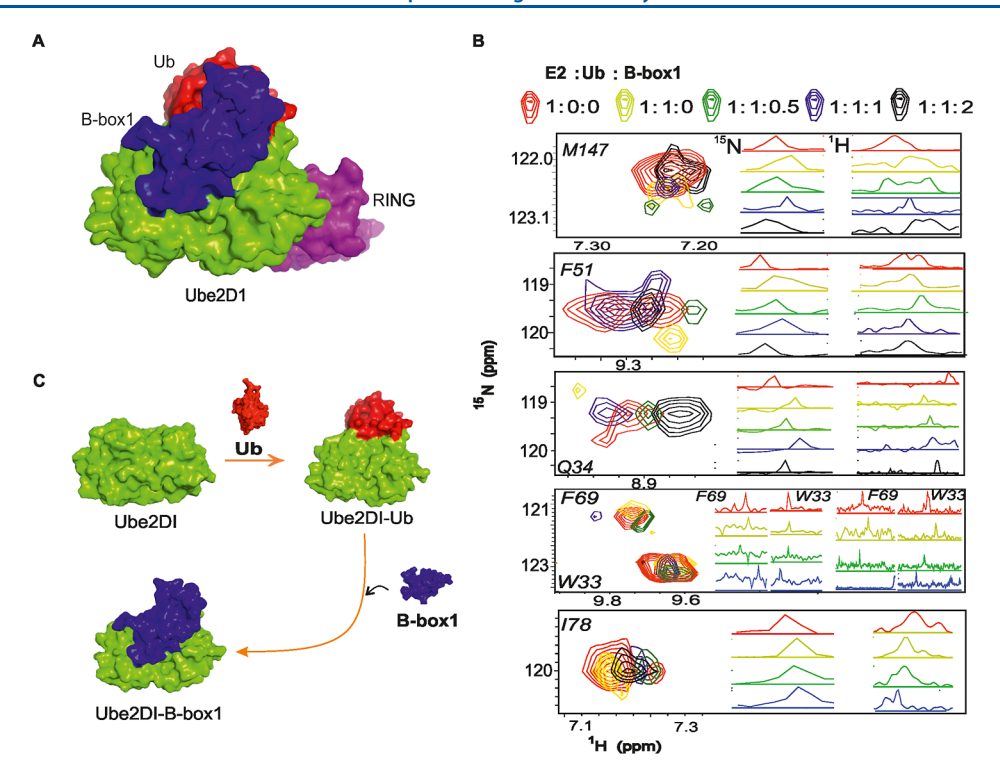


Figure 9. Binding sites of Ub and B-box1 on Ube2D1. (A) Surface representation of Ube2D1 with the noncovalent interaction sites of RING, B-box1, and ubiquitin. (B) Zoomed-in regions of the Ube2D1 ¹H-¹⁵N HSQC spectra of amino acids M147, F51, and Q34 (key residues for Ube2D1-Ub interaction) and of F69, W33, and I78 (residues involved in binding with the Ube2D1-B-box1 complex). The corresponding ¹⁵N and ¹H projections of each peak of Ube2D1 in the presence of Ub show significant changes when titrated with the B-box1 domain. The NMR titration suggests that B-box1 displaces the noncovalently bound ubiquitin, as shown in (C).

box1 domains would influence the outward orientation of loop2 and thus similar binding with the Ube2D enzyme family.

ASSOCIATED CONTENT

Supporting Information

The Supporting Information is available free of charge at https://pubs.acs.org/doi/10.1021/acs.biochem.2c00693.

NMR relaxation properties of Ube2D1; analysis of HADDOCK predicted structures; and NMR titrations of 15N-labeled Ube2D1 with B-box1 and Ub (PDF)

Accession Codes

Ubiquitin-conjugating enzyme (Ube2D1, P51668). E3-Ubiquitin protein ligase Midline-1 (MID1, O15344).

AUTHOR INFORMATION

Corresponding Author

Michael A. Massiah — Department of Chemistry, George Washington University, Washington, D.C. 20052, United States; Phone: +1-202-994-2150; Email: massiah@gwu.edu; Fax: +1-202-994-5873

Authors

Anupreet Kaur — Department of Chemistry, George Washington University, Washington, D.C. 20052, United States; orcid.org/0000-0001-9037-1128

Erin M. Gladu – Department of Chemistry, George Washington University, Washington, D.C. 20052, United States

Katharine M. Wright – Department of Chemistry, George Washington University, Washington, D.C. 20052, United States

Jessica A. Webb – Department of Chemistry, George Washington University, Washington, D.C. 20052, United States

Complete contact information is available at: https://pubs.acs.org/10.1021/acs.biochem.2c00693

Author Contributions

A.K.: NMR experimental and data analysis, isothermal titrations, and writing—review and editing. E.M.G.: thiolysis and auto-ubiquitination assays. J.A.W.: experimental work and collected NMR data. K.M.W.: experimental planning and NMR data recording. M.A.M.: conceptualization, funding acquisition, project administration, methodology, supervision, and writing—review and editing.

Notes

The authors declare no competing financial interest.

ACKNOWLEDGMENTS

The authors would like to thank Dr. Haijuan Du for help and guidance with the initial phase of this project. The work was supported in part by the National Science Foundation (MM, 1808391)

REFERENCES

(1) De Falco, F.; Cainarca, S.; Andolfi, G.; Ferrentino, R.; Berti, C.; Rodríguez Criado, G.; Rittinger, O.; Dennis, N.; Odent, S.; Rastogi, A.; Liebelt, J.; Chitayat, D.; Winter, R.; Jawanda, H.; Ballabio, A.; Franco, B.; Meroni, G. X-linked Opitz syndrome: Novel mutations in the MID1gene and redefinition of the clinical spectrum. *Am. J. Med. Genet., Part A* 2003, 120, 222–228.

(2) Opitz, J. M. The G syndrome of multiple congenital anomalies. *Birth Defects, Orig. Artic. Ser.* **1969**, *2*, 95–101.

- (3) Du, H.; Wu, K.; Didoronkute, A.; Levy, M. V.; Todi, N.; Shchelokova, A.; Massiah, M. A. MID1 catalyzes the ubiquitination of protein phosphatase 2A and mutations within its Bbox1 domain disrupt polyubiquitination of alpha4 but not of PP2Ac. *PLoS One* **2014**, *9*, No. e107428.
- (4) Short, K. M.; Cox, T. C. Subclassification of the RBCC/TRIM Superfamily Reveals a Novel Motif Necessary for Microtubule Binding. *J. Biol. Chem.* **2006**, *281*, 8970–8980.
- (5) Han, X.; Du, H.; Massiah, M. A. Detection and characterization of the in vitro e3 ligase activity of the human MID1 protein. *J. Mol. Biol.* **2011**, 407, 505–520.
- (6) Du, H.; Huang, Y.; Zaghlula, M.; Walters, E.; Cox, T. C.; Massiah, M. A. The MID1 E3 Ligase Catalyzes the Polyubiquitination of Alpha4 (α 4), a Regulatory Subunit of Protein Phosphatase 2A (PP2A). *J. Biol. Chem.* **2013**, 288, 21341–21350.
- (7) Schweiger, S.; Schneider, R. The MID1/PP2A complex: a key to the pathogenesis of Opitz BBB/G syndrome. *Bioessays* **2003**, 25, 356–366.
- (8) Janssens, V.; Goris, J. Protein phosphatase 2A: a highly regulated family of serine/threonine phosphatases implicated in cell growth and signalling. *Biochem. J.* **2001**, 353, 417–439.
- (9) Lechward, K.; Awotunde, O. S.; Swiatek, W.; Muszyńska, G. Protein phosphatase 2A: variety of forms and diversity of functions. *Acta Biochim. Pol.* **2001**, *48*, 921–933.
- (10) Liu, E.; Knutzen, C. A.; Krauss, S.; Schweiger, S.; Chiang, G. G. Control of mTORC1 signaling by the Opitz syndrome protein MID1. *Proc. Natl. Acad. Sci. U.S.A.* **2011**, *108*, 8680–8685.
- (11) Trockenbacher, A.; Suckow, V.; Foerster, J.; Winter, J.; Krauß, S.; Ropers, H. H.; Schneider, R.; Schweiger, S. MID1, mutated in Opitz syndrome, encodes an ubiquitin ligase that targets phosphatase 2A for degradation. *Nat. Genet.* **2001**, *29*, 287–294.
- (12) Kong, M.; Ditsworth, D.; Lindsten, T.; Thompson, C. B. α 4 Is an Essential Regulator of PP2A Phosphatase Activity. *Mol. Cell* **2009**, 36, 51–60.
- (13) Mita, M. M.; Mita, A.; Rowinsky, E. K. Mammalian target of rapamycin: a new molecular target for breast cancer. *Clin. Breast Cancer* **2003**, *4*, 126–137.
- (14) McConnell, J. L.; Watkins, G. R.; Soss, S. E.; Franz, H. S.; McCorvey, L. R.; Spiller, B. W.; Chazin, W. J.; Wadzinski, B. E. Alpha4 is a ubiquitin-binding protein that regulates protein serine/threonine phosphatase 2A ubiquitination. *Biochemistry* **2010**, 49, 1713–1718.
- (15) Jiang, Y.; Broach, J. R. Tor proteins and protein phosphatase 2A reciprocally regulate Tap42 in controlling cell growth in yeast. *EMBO J.* **1999**, *18*, 2782–2792.
- (16) Rao, R. D.; Buckner, J. C.; Sarkaria, J. N. Mammalian target of rapamycin (mTOR) inhibitors as anti-cancer agents. *Curr. Cancer Drug Targets* **2004**, *4*, 621–635.
- (17) Schweiger, S.; Dorn, S.; Fuchs, M.; Köhler, A.; Matthes, F.; Müller, E.-C.; Wanker, E.; Schneider, R.; Krauß, S. The E3 ubiquitin ligase MID1 catalyzes ubiquitination and cleavage of Fu. *J. Biol. Chem.* **2014**, 289, 31805–31817.
- (18) Borden, K. L. RING fingers and B-boxes: zinc-binding protein-protein interaction domains. *Biochem. Cell Biol.* **1998**, *76*, 351–358.
- (19) Massiah, M. A.; Simmons, B. N.; Short, K. M.; Cox, T. C. Solution structure of the RBCC/TRIM B-box1 domain of human MID1: B-box with a RING. *J. Mol. Biol.* **2006**, 358, 532–545.
- (20) Massiah, M. A.; Matts, J. A.; Short, K. M.; Simmons, B. N.; Singireddy, S.; Yi, Z.; Cox, T. C. Solution Structure of the MID1 B-box2 CHC(D/C)C2H2 Zinc-binding Domain: Insights into an Evolutionarily Conserved RING Fold. *J. Mol. Biol.* **2007**, *369*, 1–10.
- (21) Gangappa, S. N.; Botto, J. F. The BBX family of plant transcription factors. *Trends Plant Sci.* **2014**, *19*, 460–470.
- (22) Khanna, R.; Kronmiller, B.; Maszle, D. R.; Coupland, G.; Holm, M.; Mizuno, T.; Wu, S. H. The Arabidopsis B-box zinc finger family. *Plant Cell* **2009**, *21*, 3416–3420.
- (23) Pickart, C. M. Ubiquitin biology: an old dog learns an old trick. *Nat. Cell Biol.* **2000**, *2*, E139–E140.

- (24) Pickart, C. M. Mechanisms underlying ubiquitination. *Annu. Rev. Biochem.* **2001**, *70*, 503–533.
- (25) Pickart, C. M.; Fushman, D. Polyubiquitin chains: polymeric protein signals. *Curr. Opin. Chem. Biol.* **2004**, *8*, 610–616.
- (26) Jackson, P. K.; Eldridge, A. G.; Freed, E.; Furstenthal, L.; Hsu, J. Y.; Kaiser, B. K.; Reimann, J. D. The lore of the RINGs: substrate recognition and catalysis by ubiquitin ligases. *Trends Cell Biol.* **2000**, 10, 429–439.
- (27) Raasi, S.; Pickart, C. M. Ubiquitin chain synthesis. *Methods Mol. Biol.* 2005, 301, 47–55.
- (28) Das, R.; Liang, Y. H.; Mariano, J.; Li, J.; Huang, T.; King, A.; Tarasov, S. G.; Weissman, A. M.; Ji, X.; Byrd, R. A. Allosteric regulation of E2:E3 interactions promote a processive ubiquitination machine. *EMBO J.* **2013**, 32, 2504–2516.
- (29) Plechanovová, A.; Jaffray, E. G.; Tatham, M. H.; Naismith, J. H.; Hay, R. T. Structure of a RING E3 ligase and ubiquitin-loaded E2 primed for catalysis. *Nature* **2012**, 489, 115–120.
- (30) Huang, A.; de Jong, R. N.; Wienk, H.; Winkler, G. S.; Timmers, H. T.; Boelens, R. E2-c-Cbl recognition is necessary but not sufficient for ubiquitination activity. *J. Mol. Biol.* **2009**, 385, 507–519.
- (31) Bentley, M. L.; Corn, J. E.; Dong, K. C.; Phung, Q.; Cheung, T. K.; Cochran, A. G. Recognition of UbcH5c and the nucleosome by the Bmi1/Ring1b ubiquitin ligase complex. *EMBO J.* **2011**, *30*, 3285–3297.
- (32) Dominguez, C.; Bonvin, A. M.; Winkler, G. S.; van Schaik, F. M.; Timmers, H. T.; Boelens, R. Structural model of the UbcH5B/CNOT4 complex revealed by combining NMR, mutagenesis, and docking approaches. *Structure* **2004**, *12*, 633–644.
- (33) Dou, H.; Buetow, L.; Sibbet, G. J.; Cameron, K.; Huang, D. T. BIRC7-E2 ubiquitin conjugate structure reveals the mechanism of ubiquitin transfer by a RING dimer. *Nat. Struct. Mol. Biol.* **2012**, *19*, 876–883
- (34) Mace, P. D.; Linke, K.; Feltham, R.; Schumacher, F. R.; Smith, C. A.; Vaux, D. L.; Silke, J.; Day, C. L. Structures of the cIAP2 RING domain reveal conformational changes associated with ubiquitin-conjugating enzyme (E2) recruitment. *J. Biol. Chem.* **2008**, 283, 31633–31640.
- (35) Pruneda, J. N.; Littlefield, P. J.; Soss, S. E.; Nordquist, K. A.; Chazin, W. J.; Brzovic, P. S.; Klevit, R. E. Structure of an E3:E2~Ub Complex Reveals an Allosteric Mechanism Shared among RING/Ubox Ligases. *Mol. Cell* **2012**, *47*, 933–942.
- (36) Das, R.; Liang, Y. H.; Mariano, J.; Li, J.; Huang, T.; King, A.; Tarasov, S. G.; Weissman, A. M.; Ji, X.; Byrd, R. A. Allosteric regulation of E2:E3 interactions promote a processive ubiquitination machine. *EMBO J.* **2013**, 32, 2504–2516.
- (37) Özkan, E.; Yu, H.; Deisenhofer, J. Mechanistic insight into the allosteric activation of a ubiquitin-conjugating enzyme by RING-type ubiquitin ligases. *Proc. Natl. Acad. Sci. U.S.A.* **2005**, *102*, 18890–18895.
- (38) Wright, K. M.; Wu, K.; Babatunde, O.; Du, H.; Massiah, M. A. XLOS-observed mutations of MID1 Bbox1 domain cause domain unfolding. *PLoS One* **2014**, *9*, No. e107537.
- (39) Wright, K. M.; Du, H.; Massiah, M. A. Structural and functional observations of the P151L MID1 mutation reveal alpha4 plays a significant role in X-linked Opitz Syndrome. *FEBS J.* **2017**, 284, 2183–2193.
- (40) Nguyen, L.; Plafker, K. S.; Starnes, A.; Cook, M.; Klevit, R. E.; Plafker, S. M. The ubiquitin-conjugating enzyme, UbcM2, is restricted to monoubiquitylation by a two-fold mechanism that involves backside residues of E2 and Lys48 of ubiquitin. *Biochemistry* **2014**, 53, 4004–4014.
- (41) Starita, L. M.; Pruneda, J. N.; Lo, R. S.; Fowler, D. M.; Kim, H. J.; Hiatt, J. B.; Shendure, J.; Brzovic, P. S.; Fields, S.; Klevit, R. E. Activity-enhancing mutations in an E3 ubiquitin ligase identified by high-throughput mutagenesis. *Proc. Natl. Acad. Sci. U.S.A.* **2013**, *110*, No. E1263.
- (42) Stevens, R. V.; Esposito, D.; Rittinger, K. Characterisation of class VI TRIM RING domains: linking RING activity to C-terminal domain identity. *Life Sci. Alliance* **2019**, *2*, No. e201900295.

- (43) Behera, A. P.; Naskar, P.; Agarwal, S.; Banka, P. A.; Poddar, A.; Datta, A. B. Structural insights into the nanomolar affinity of RING E3 ligase ZNRF1 for Ube2N and its functional implications. *Biochem. J.* 2018, 475, 1569–1582.
- (44) Delaglio, F.; Grzesiek, S.; Vuister, G. W.; Zhu, G.; Pfeifer, J.; Bax, A. NMRPipe: a multidimensional spectral processing system based on UNIX pipes. *J. Biomol. NMR* **1995**, *6*, 277.
- (45) Vranken, W. F.; Boucher, W.; Stevens, T. J.; Fogh, R. H.; Pajon, A.; Llinas, M.; Ulrich, E. L.; Markley, J. L.; Ionides, J.; Laue, E. D. The CCPN data model for NMR spectroscopy: development of a software pipeline. *Proteins: Struct., Funct., Bioinf.* 2005, 59, 687–696.
- (46) Lee, W.; Tonelli, M.; Markley, J. L. NMRFAM-SPARKY: enhanced software for biomolecular NMR spectroscopy. *Bioinformatics* **2015**, *31*, 1325–1327.
- (47) de Vries, S. J.; van Dijk, M.; Bonvin, A. M. The HADDOCK web server for data-driven biomolecular docking. *Nat. Protoc.* **2010**, *5*, 883–897.
- (48) Dominguez, C.; Boelens, R.; Bonvin, A. M. HADDOCK: A Protein—Protein Docking Approach Based on Biochemical or Biophysical Information. J. Am. Chem. Soc. 2003, 125, 1731–1737.
- (49) Massiah, M. A.; Simmons, B. N.; Short, K. M.; Cox, T. C. Solution structure of the RBCC/TRIM B-box1 domain of human MID1: B-box with a RING. *J. Mol. Biol.* **2006**, 358, 532–545.
- (50) Tao, H.; Simmons, B. N.; Singireddy, S.; Jakkidi, M.; Short, K. M.; Cox, T. C.; Massiah, M. A. Structure of the MID1 Tandem B-Boxes Reveals an Interaction Reminiscent of Intermolecular Ring Heterodimers, *Biochemistry* **2008**, *47*, 2450–2457.
- (51) Gladu, E. M.; Sayed, I.; Massiah, M. A. Review of the Structural Basis of Human E2 Conjugating Enzymes in Complexed with RING E3 Ligases. *Hydrolases*; IntechOpen, 2022, 105.
- (52) Stewart, M. D.; Ritterhoff, T.; Klevit, R. E.; Brzovic, P. S. E2 enzymes: more than just middle men. *Cell Res.* **2016**, *26*, 423–440.
- (53) Christensen, D. E.; Brzovic, P. S.; Klevit, R. E. E2-BRCA1 RING interactions dictate synthesis of mono- or specific polyubiquitin chain linkages. *Nat. Struct. Mol. Biol.* **2007**, *14*, 941–948.
- (54) Chen, A.; Kleiman, F. E.; Manley, J. L.; Ouchi, T.; Pan, Z.-Q. Autoubiquitination of the BRCA1·BARD1 RING Ubiquitin Ligase. *J. Biol. Chem.* **2002**, *277*, 22085–22092.
- (55) Fang, S.; Jensen, J. P.; Ludwig, R. L.; Vousden, K. H.; Weissman, A. M. Mdm2 is a RING finger-dependent ubiquitin protein ligase for itself and p53. *J. Biol. Chem.* **2000**, *275*, 8945–8951.
- (56) Han, X.; Du, H.; Massiah, M. A. Detection and characterization of the in vitro e3 ligase activity of the human MID1 protein. *J. Mol. Biol.* **2011**, 407, 505–520.
- (57) Du, H.; Huang, Y.; Zaghlula, M.; Walters, E.; Cox, T. C.; Massiah, M. A. The MID1 E3 Ligase Catalyzes the Polyubiquitination of Alpha4 (α 4), a Regulatory Subunit of Protein Phosphatase 2A (PP2A). *J. Biol. Chem.* **2013**, 288, 21341–21350.
- (58) Wenzel, D. M.; Lissounov, A.; Brzovic, P. S.; Klevit, R. E. UBCH7 reactivity profile reveals parkin and HHARI to be RING/HECT hybrids. *Nature* **2011**, *474*, 105–108.
- (59) Mace, P. D.; Linke, K.; Feltham, R.; Schumacher, F.-R.; Smith, C. A.; Vaux, D. L.; Silke, J.; Day, C. L. Structures of the cIAP2 RING domain reveal conformational changes associated with ubiquitin-conjugating enzyme (E2) recruitment. *J. Biol. Chem.* **2008**, 283, 31633–31640.
- (60) Liew, C. W.; Sun, H.; Hunter, T.; Day, C. L. RING domain dimerization is essential for RNF4 function. *Biochem. J.* **2010**, *431*, 23–29.
- (61) Dou, H.; Buetow, L.; Sibbet, G. J.; Cameron, K.; Huang, D. T. BIRC7-E2 ubiquitin conjugate structure reveals the mechanism of ubiquitin transfer by a RING dimer. *Nat. Struct. Mol. Biol.* **2012**, *19*, 876–883.
- (62) Ohi, M. D.; Vander Kooi, C. W.; Rosenberg, J. A.; Chazin, W. J.; Gould, K. L. Structural insights into the U-box, a domain associated with multi-ubiquitination. *Nat. Struct. Mol. Biol.* **2003**, *10*, 250–255.
- (63) Vander Kooi, C. W.; Ohi, M. D.; Rosenberg, J. A.; Oldham, M. L.; Newcomer, M. E.; Gould, K. L.; Chazin, W. J. The Prp19 U-box Crystal Structure Suggests a Common Dimeric Architecture for a

- Class of Oligomeric E3 Ubiquitin Ligases, *Biochemistry* **2006**, 45, 121–130.
- (64) Huang, A.; de Jong, R. N.; Wienk, H.; Winkler, G. S.; Timmers, H. T. M.; Boelens, R. E2-c-Cbl Recognition Is Necessary but not Sufficient for Ubiquitination Activity. *J. Mol. Biol.* **2009**, 385, 507–519
- (65) Das, R.; Mariano, J.; Tsai, Y. C.; Kalathur, R. C.; Kostova, Z.; Li, J.; Tarasov, S. G.; McFeeters, R. L.; Altieri, A. S.; Ji, X.; Byrd, R. A.; Weissman, A. M. Allosteric activation of E2-RING finger-mediated ubiquitylation by a structurally defined specific E2-binding region of gp78. *Mol. Cell* **2009**, *34*, 674–685.
- (66) Buetow, L.; Gabrielsen, M.; Anthony, N. G.; Dou, H.; Patel, A.; Aitkenhead, H.; Sibbet, G. J.; Smith, B. O.; Huang, D. T. Activation of a Primed RING E3-E2-Ubiquitin Complex by Non-Covalent Ubiquitin. *Mol. Cell* **2015**, *58*, 297–310.
- (67) Sarkar, S.; Behera, A. P.; Borar, P.; Banka, P. A.; Datta, A. B. Designing active RNF4 monomers by introducing a tryptophan: avidity towards E2~Ub conjugates dictates the activity of ubiquitin RING E3 ligases. *Biochem. J.* **2019**, *476*, 1465–1482.
- (68) Brzovic, P. S.; Lissounov, A.; Christensen, D. E.; Hoyt, D. W.; Klevit, R. E. A UbcH5/ubiquitin noncovalent complex is required for processive BRCA1-directed ubiquitination. *Mol. Cell* **2006**, *21*, 873–880.
- (69) Li, S.; Liang, Y.-H.; Mariano, J.; Metzger, M. B.; Stringer, D. K.; Hristova, V. A.; Li, J.; Randazzo, P. A.; Tsai, Y. C.; Ji, X.; Weissman, A. M. Insights into ubiquitination from the unique clamp-like binding of the RING E3 AO7 to the E2 UbcH5B. *J. Biol. Chem.* **2015**, 290, 30225–30239.
- (70) Houben, K.; Dominguez, C.; van Schaik, F. M.; Timmers, H. T. M.; Bonvin, A. M.; Boelens, R. Solution structure of the ubiquitin-conjugating enzyme UbcH5B. *J. Mol. Biol.* **2004**, 344, 513–526.
- (71) Huang, X.; de Vera, I. M. S.; Veloro, A. M.; Rocca, J. R.; Simmerling, C.; Dunn, B. M.; Fanucci, G. E. Backbone 1H, 13C, and 15N chemical shift assignment for HIV-1 protease subtypes and multi-drug resistant variant MDR 769. *Biomol. NMR Assignments* 2013, 7, 199–202.
- (72) Mercier, P.; Lewis, M. J.; Hau, D. D.; Saltibus, L. F.; Xiao, W.; Spyracopoulos, L. Structure, interactions, and dynamics of the RING domain from human TRAF6. *Protein Sci.* **2007**, *16*, 602–614.
- (73) Bijlmakers, M. J.; Teixeira, J. M.; Boer, R.; Mayzel, M.; Puig-Sàrries, P.; Karlsson, G.; Coll, M.; Pons, M.; Crosas, B. A C2HC zinc finger is essential for the RING-E2 interaction of the ubiquitin ligase RNF125. *Sci. Rep.* **2016**, *6*, 29232.
- (74) Bijlmakers, M.-J.; Teixeira, J.; Boer, R.; Mayzel, M.; Puig-Sàrries, P.; Karlsson, G.; Coll, M.; Pons, M.; Crosas, B. A C2HC zinc finger is essential for the RING-E2 interaction of the ubiquitin ligase RNF125. *Sci. Rep.* **2016**, *6*, 29232.
- (75) Chakrabarti, K. S.; Li, J.; Das, R.; Byrd, R. A. Conformational Dynamics and Allostery in E2:E3 Interactions Drive Ubiquitination: gp78 and Ube2g2. *Structure* **2017**, *25*, 794–805.
- (76) Ju, T.; Bocik, W.; Majumdar, A.; Tolman, J. R. Solution structure and dynamics of human ubiquitin conjugating enzyme Ube2g2. *Proteins: Struct., Funct., Bioinf.* **2010**, *78*, 1291–1301.
- (77) Rout, M. K.; Hodge, C. D.; Markin, C. J.; Xu, X.; Glover, J. M.; Xiao, W.; Spyracopoulos, L. Stochastic gate dynamics regulate the catalytic activity of ubiquitination enzymes. *J. Am. Chem. Soc.* **2014**, *136*, 17446–17458.
- (78) Laskowski, R. A. PDBsum new things. *Nucleic Acids Res.* **2009**, 37, D355–D359.
- (79) Nakasone, M. A.; Majorek, K. A.; Gabrielsen, M.; Sibbet, G. J.; Smith, B. O.; Huang, D. T. Structure of UBE2K—Ub/E3/polyUb reveals mechanisms of K48-linked Ub chain extension. *Nat. Chem. Biol.* **2022**, *18*, 422.
- (80) Wright, K. M.; Du, H.; Massiah, M. A. Structural and functional observations of the P151L MID1 mutation reveal alpha4 plays a significant role in X-linked Opitz Syndrome. *FEBS J.* **2017**, 284, 2183–2193.
- (81) Lips, C.; Ritterhoff, T.; Weber, A.; Janowska, M. K.; Mustroph, M.; Sommer, T.; Klevit, R. E. Who with whom: functional

- coordination of E2 enzymes by RING E3 ligases during polyubiquitylation. *EMBO J.* **2020**, *39*, No. e104863.
- (82) Christensen, D. E.; Brzovic, P. S.; Klevit, R. E. E2-BRCA1 RING interactions dictate synthesis of mono- or specific polyubiquitin chain linkages. *Nat. Struct. Mol. Biol.* **2007**, *14*, 941–948.
- (83) Dove, K. K.; Kemp, H. A.; Di Bona, K. R.; Reiter, K. H.; Milburn, L. J.; Camacho, D.; Fay, D. S.; Miller, D. L.; Klevit, R. E. Two functionally distinct E2/E3 pairs coordinate sequential ubiquitination of a common substrate in Caenorhabditis elegans development. *Proc. Natl. Acad. Sci. U.S.A.* 2017, 114, E6576–E6584.
- (84) Pruneda, J. N.; Littlefield, P. J.; Soss, S. E.; Nordquist, K. A.; Chazin, W. J.; Brzovic, P. S.; Klevit, R. E. Structure of an E3:E2~Ub Complex Reveals an Allosteric Mechanism Shared among RING/U-box Ligases. *Mol. Cell* **2012**, *47*, 933–942.
- (85) Buetow, L.; Gabrielsen, M.; Anthony, N. G.; Dou, H.; Patel, A.; Aitkenhead, H.; Sibbet, G. J.; Smith, B. O.; Huang, D. T. Activation of a primed RING E3-E2-ubiquitin complex by non-covalent ubiquitin. *Mol. Cell* **2015**, *58*, 297–310.
- (86) Massiah, M. A. Zinc-binding B-box domains with RING folds serve critical roles in the protein ubiquitination pathways in plants and animals. *Ubiquitin Proteasome System-Current Insights into Mechanism Cellular Regulation and Disease*; Intechopen, 2019
- (87) Zhao, Y.; Zeng, C.; Massiah, M. A. Molecular dynamics simulation reveals insights into the mechanism of unfolding by the A130T/V mutations within the MID1 zinc-binding Bbox1 domain. *PLoS One* **2015**, *10*, No. e0124377.
- (88) Metzger, M. B.; Pruneda, J. N.; Klevit, R. E.; Weissman, A. M. RING-type E3 ligases: master manipulators of E2 ubiquitin-conjugating enzymes and ubiquitination. *Biochim. Biophys. Acta* **2014**, *1843*, 47–60.
- (89) Buetow, L.; Huang, D. T. Structural insights into the catalysis and regulation of E3 ubiquitin ligases. *Nat. Rev. Mol. Cell Biol.* **2016**, 17, 626–642.
- (90) Linke, K.; Mace, P.; Smith, C.; Vaux, D.; Silke, J.; Day, C. L. Structure of the MDM2/MDMX RING domain heterodimer reveals dimerization is required for their ubiquitylation in trans. *Cell Death Differ.* **2008**, *15*, 841–848.
- (91) Pan, Y.; Chen, J. MDM2 promotes ubiquitination and degradation of MDMX. *Mol. Cell Biol.* **2003**, 23, 5113–5121.
- (92) Brzovic, P. S.; Rajagopal, P.; Hoyt, D. W.; King, M. C.; Klevit, R. E. Structure of a BRCA1-BARD1 heterodimeric RING-RING complex. *Nat. Struct. Biol.* **2001**, *8*, 833–837.
- (93) Mallery, D. L.; Vandenberg, C. J.; Hiom, K. Activation of the E3 ligase function of the BRCA1/BARD1 complex by polyubiquitin chains. *EMBO J.* **2002**, *21*, 6755–6762.
- (94) Linke, K.; Mace, P. D.; Smith, C. A.; Vaux, D. L.; Silke, J.; Day, C. L. Structure of the MDM2/MDMX RING domain heterodimer reveals dimerization is required for their ubiquitylation in trans. *Cell Death Differ.* **2008**, *15*, 841–848.

□ Recommended by ACS

Addressing Transcriptional Dysregulation in Cancer through CDK9 Inhibition

Mohammed A. Toure and Angela N. Koehler

FEBRUARY 28, 2023

BIOCHEMISTRY

READ 🗹

Biochemical Studies of Systemic Lupus Erythematosus-Associated Mutations in Nonreceptor Tyrosine Kinases Ack1 and Brk

Yagmur Kan, W. Todd Miller, et al.

FEBRUARY 28, 2023

BIOCHEMISTRY

READ

Transport Mechanism for Nuclear Localization of Irradiation-Activated EGFR Measured by Single-Molecule Pull-Down Assay

Jiwon Oh, Seung Wook Ham, et al.

FEBRUARY 06, 2023

BIOCHEMISTRY

READ 🗹

Unfolding and Aggregation Pathways of Variable Domains from Immunoglobulin Light Chains

Yadira Meunier-Carmenate, Carlos Amero, et al.

FEBRUARY 21, 2023

BIOCHEMISTRY

READ 🗹

Get More Suggestions >